ChemComm

COMMUNICATION

Cite this: *Chem. Commun.*, 2017, 53, 7041

Received 15th March 2017,
Accepted 6th June 2017

DOI: 10.1039/c7cc01985h

rsc.li/chemcomm

Tracking thermal-induced amorphization of a zeolitic imidazolate framework *via* synchrotron *in situ* far-infrared spectroscopy†

Matthew R. Ryder,[ab] Thomas D. Bennett,[c] Chris S. Kelley,[b] Mark D. Frogley,[b] Gianfelice Cinque[b] and Jin-Chong Tan*[a]

We present the first use of *in situ* far-infrared spectroscopy to analyze the thermal amorphization of a zeolitic imidazolate framework material. We explain the nature of vibrational motion changes during the amorphization process and reveal new insights into the effect that temperature has on the Zn–N tetrahedra.

Vibrational spectroscopy has been shown to be an excellent method of analyzing framework materials and gaining a better understanding of their molecular structure. The mid-infrared (MIR) region of the vibrational spectra is related to the local characteristic vibrations (*e.g.* localized bond stretching and bending) and is therefore of limited interest for providing information regarding lattice dynamics of a specific framework. However, there has recently been a strong focus on the framework specific vibrational motions located in the far-infrared (FIR) region (<700 cm^{-1}), which have been shown to reveal the nature of quasi-localized and collective modes.

One group of framework materials exhibiting a particularly rich variety of collective vibrational motions are metal–organic frameworks (MOFs), which are a topical class of hybrid (inorganic–organic) crystalline materials. Their nanoscale pore structures and long-range order have attracted significant scientific and industrial interest, which originates from their wide range of potential applications including, carbon sequestration, photonics and microelectronics, and drug encapsulation and delivery.[1] The diverse structural behavior of MOFs[2] results in the FIR region of the vibrational spectra providing a gateway to understanding the physical behavior and underlying flexibility of these highly promising next-generation functional materials.

We have shown that inelastic neutron scattering (INS) and synchrotron-based FIR spectroscopy, in conjunction with *ab initio* density functional theory (DFT) can be used to explain these framework specific motions.[3] Specifically, we related quasi-local vibrations to the deformation of the organic linkers and Zn-based coordination polyhedra (ZnN_4) in zeolitic imidazolate frameworks (ZIFs),[4] and linked them to various physical phenomena, including "gate-opening", "breathing" and shear destabilization modes.[3] We also reported molecular rotational dynamics, trampoline-like vibrational motions, and demonstrated how collective vibrations can be connected to the elasticity and mechanical stability of the framework structure, revealing the origin of auxeticity (negative Poisson's ratio),[5] in the copper paddle-wheel MOF, HKUST-1.[6] Unlike *in situ* MIR spectroscopy,[7] which can be performed *via* benchtop equipment, detailed characterization of the FIR region *in situ* requires a more sophisticated experimental setup, explaining the relative absence of reports to date.

The structural dynamics of MOFs, at the molecular level, are of increasing importance. For example, phase transitions in ZIF-7 upon exchange of guest molecules and ZIF-8 upon gas adsorption have been ascribed to "breathing" and "gate-opening" mechanisms respectively.[3,8] Another topical MOF material, MIL-53, has also been reported to undergo transitions upon cooling.[9]

In this work, we have advanced the use of FIR vibrational spectroscopy to follow the *in situ* thermal transformations of ZIF-4, which has the chemical composition $Zn(Im)_2$ [Im = imidazolate, $C_3H_3N_2^-$]. The framework was selected, as it has been shown to demonstrate significant flexibility regarding its phase transition ability.[10] It is known to amorphize to a structure called a-ZIF at approximately 573 K, which is separate from the solvent induced collapse of ZIFs. The amorphous structure is reported to be a continuous random network analogous to that of amorphous silica (a-SiO_2).[10,11] Upon further heating (above 673 K) a-ZIF recrystallizes into the higher symmetry dense structure, ZIF-zni.[10] Dense ZIF-zni is the lower energy of the two crystalline structures[12] but only becomes thermally accessible above 673 K. ZIF-zni has an identical chemical composition to ZIF-4. However, their crystal symmetries, network topologies and geometrical

[a] *Multifunctional Materials and Composites (MMC) Laboratory, Department of Engineering Science, University of Oxford, Parks Road, Oxford OX1 3PJ, UK. E-mail: jin-chong.tan@eng.ox.ac.uk; Tel: +44 1865 273925*

[b] *Diamond Light Source, Harwell Campus, Chilton, Oxford OX11 0DE, UK*

[c] *Department of Materials Science and Metallurgy, University of Cambridge, Cambridge CB3 0FS, UK*

† Electronic supplementary information (ESI) available. See DOI: 10.1039/c7cc01985h

parameters are remarkably different.[10,13] ZIF-4 has also been reported to undergo a discontinuous porous to dense phase transition upon cooling to under 140 K, due to cooperative rotations of the organic linkers.[14] The temperature ranges of these phases are indicated in Fig. 3 by ZIF-4 (LT/HT). For comparison, we have also investigated the thermal effects on the vibrational spectra of ZIF-8 (whose linker is mIm = 2-methylimidazolate), which does not amorphize thermally.[15] It is worth noting that these materials can also amorphize through other sources of external stimuli, such as pressure[16] and mechanical impact.[17] However, it has been suggested that the mechanisms for the various routes to amorphization are different, with a shear instability being the likely cause of the mechanically induced amorphization.[18] The thermal-induced amorphization route of ZIFs is currently a phenomenon only witnessed for ZIF structures possessing the unsubstituted imidazole (Im) linker. We have, therefore, used the results of this work to postulate a reason for this observation and propose in this communication an empirical measure to quantify the structural flexibility determining the likelihood of temperature enabled amorphization.

The experimental spectra were obtained using a novel setup recently commissioned utilizing a Bruker Vertex 80V Fourier Transform IR (FTIR) Interferometer, to provide *in situ* FIR data using a synchrotron radiation source (Fig. 1). The novelty of the setup was the introduction of an accurate temperature control, *via* a nitrogen purged Linkam cell and a Hyperion 3000 microscope.[19] A more detailed description of the experimental setup is available in the ESI.†

We know from our previous work on the low-energy vibrations of ZIF materials[3] that there are three sources of vibrational motion located in the spectral region below 700 cm^{-1}: (i) aromatic ring deformations; (ii) ZnN_4 tetrahedra deformations; (iii) framework-specific collective motions.

We have confirmed our previous work, demonstrating that the peaks relating to the ring deformations of the Im organic linkers in ZIF-4, a-ZIF and ZIF-zni are all present at approximately 640–700 cm^{-1}, along with the universally shared Zn–N bond stretching motion, specifically originating from the compliance of $Zn(Im)_4$ tetrahedra, which is again positioned at 265–325 cm^{-1} as expected (Fig. 2).[3]

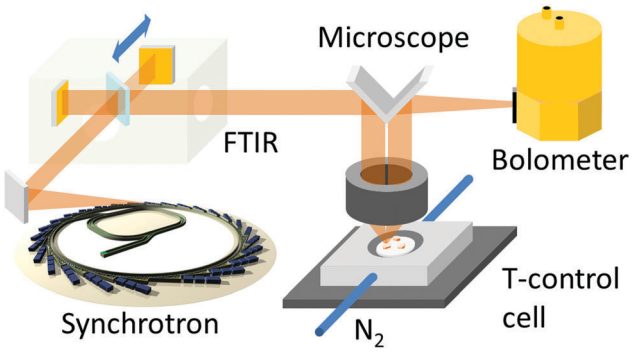

Fig. 1 Schematic of the novel experimental setup used for the *in situ* far-IR spectroscopy study conducted at the B22 beamline (MIRIAM) at Diamond Light Source.

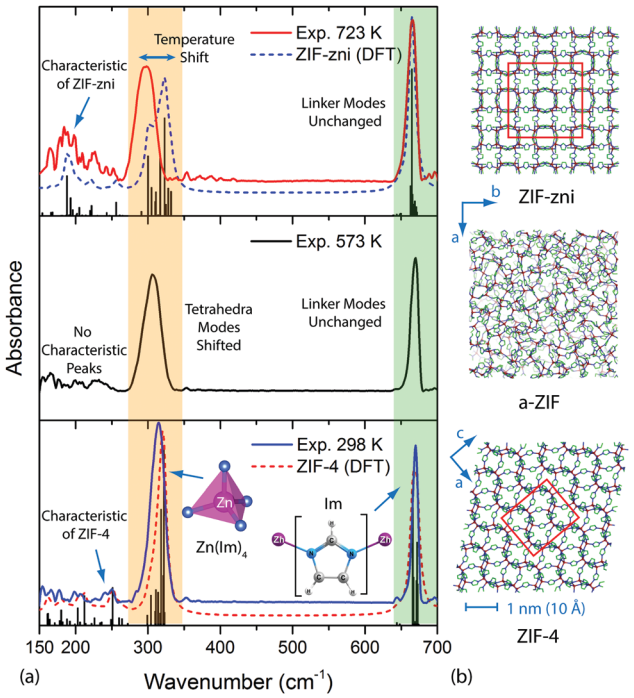

Fig. 2 (a) IR spectra in the region of 150–700 cm^{-1}, showing the spectral changes observed at 298, 573 and 723 K. The red and blue dotted lines are the theoretical ZIF-4 and ZIF-zni spectra obtained from DFT (comparable to 0 K). The modes relating to the Zn–N deformations of the $Zn(Im)_4$ tetrahedra and the deformations of the aromatic imidazole (Im) linkers are highlighted. (b) Framework structures adapted from ref. 10 of ZIF-4, a-ZIF and ZIF-zni are shown for clarity, with the unit cells of the two crystalline phases highlighted in red.

Unsurprisingly we do not see any significant effect on the peaks relating to the organic linkers, as the structurally rigid Im linkers do not strain significantly upon heating, structural amorphization, or recrystallization into ZIF-zni. Changes to the peaks at approximately 323 cm^{-1} (assuming zero thermal effects, calculated *via* DFT) are however pronounced and include a temperature induced spectral shift and are related to the Zn–N stretching modes of the ZnN_4 tetrahedra deformation in $Zn(Im)_4$. These vibrational modes are expected to be sufficiently anharmonic to show a red shift as a result of the thermal stimulus (upon heating) allowing for increased flexibility in the deformation of the $Zn(Im)_4$ tetrahedra. Due to these modes being independent of the specific framework, yet still the result of a cluster-like moiety, they may be considered as quasi-delocalized and if true should, obey a Bose–Einstein distribution.[20] The exact Bosonic nature of the phenomenon would require further investigation. However, it can be seen that the frequency shift (Fig. 3) does appear to obey well the following relation, based on Bose–Einstein statistics:

$$\nu(T) = \nu_0 - \frac{X_R T_C}{e^{\frac{T_C}{T}} - 1}, \quad \text{where} \quad T_C = \frac{h\nu_0}{k_B}$$

where ν_0 is the frequency of the mode at zero temperature (calculated *via* DFT); T is the temperature that the experimental spectra were obtained at; T_C is the vibrational temperature, related to the energy of the particular mode, obtained from

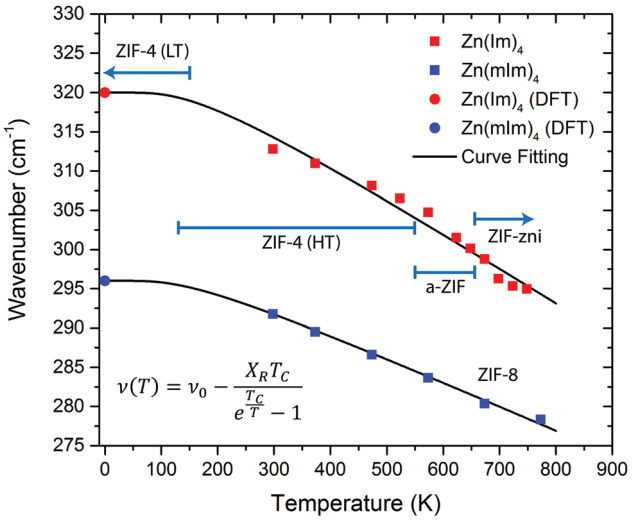

Fig. 3 Temperature dependence of the $Zn(Im)_4$ and $Zn(mIm)_4$ tetrahedra deformation modes, hence explaining the disparity between the theoretical ZIF-zni spectra and the experimental obtained at 723 K. The thermal range of each structure has been highlighted for clarity.

statistical thermodynamics, *via* the use of the Planck constant (h) and the Boltzmann constant (k_B); and a curve fitting variable, X_R, which could be described as a thermally-induced spectral shift coefficient, as we speculate the value is linked to the specific M–X polyhedral deformation, present in each distinct polyhedral environment. We expect the value of X_R to be dependent on both the type of metal and importantly the linker involved. Our current work gives the value of X_R to be 0.045 cm^{-1} K^{-1} (R^2 = 0.970) for the $Zn(Im)_4$ tetrahedral deformations in ZIF-4. We also see an increase in the gradient of the data points beyond the curve fitted for ZIF-4. This is due to the presence of the amorphous a-ZIF structure. This is confirmed by the gradient decreasing at higher temperature due to the energetically more stable ZIF-zni phase. If the value of X_R is essentially an indication of how flexible the M–X polyhedral environment is under thermal stimuli, prior to amorphization, then we could postulate that MOF structures that demonstrate a higher value of X_R could be more susceptible to thermal-induced amorphisation, as a more flexible M–X polyhedral environment would intuitively increase the probability of framework amorphisation. In the case of ZIF materials, this would be the unsubstituted $Zn(Im)_4$ containing frameworks, which all show thermal-induced amorphisation. To support this hypothesis, we investigated the value of X_R for ZIF-8, which is well accepted not to amorphize thermally.[15] Importantly, the linker is different, 2-methylimidazole (mIm), so we could provide another value of X_R, this time applied to $Zn(mIm)_4$ tetrahedral deformations. The resultant value for ZIF-8 is 0.032 cm^{-1} K^{-1} (R^2 = 0.995), hence supporting the idea that a lower value of X_R could imply an increased thermal stability to amorphization. This is most likely a direct result of the increased steric contribution from the substituted linkers, translating into a more rigid M–X polyhedra. This is of course still a postulation and the numerical evidence is limited. However, the increased flexibility in the polyhedral motion is logically linked to the structural stability, and, we show compelling evidence in this work that the polyhedral deformation (flexibility) upon thermal stimulus can be precisely monitored using *in situ* far-IR synchrotron spectroscopy.

Table 1 Nature of the IR-active modes in the 150–700 cm^{-1} region

Structure	Spectral region (cm^{-1})	Description of vibrational motion
ZIF-4 ZIF-zni	160–275 155–280	4-Membered and 6-membered ring deformation; ligand rotation (rocking); N–Zn–N bending and Zn–N stretching (tetrahedral deformation)
ZIF-4 ZIF-zni	295–325 290–330	Zn–N stretching (belonging to ZnN_4 tetrahedra)
ZIF-4 and ZIF-zni	640–700	Aromatic ring deformation and torsion modes (in-plane and out-of-plane)

Moving on to the distinction between the two crystalline structures, the final modes observed are the collective vibrational motions that are specific to the framework structure and symmetry. These modes are located in the region of 155–280 cm^{-1} (Fig. 2) and are all due to specific motions involving the 4-membered and 6-membered ring deformations, simultaneously coupled with ligand rocking.[3] Due to the differences in crystal packing and symmetry between ZIF-4 and ZIF-zni the intensities of the peaks in this region are distinct to each framework. For example, in ZIF-4 we observe a broader distribution of modes due to the lower symmetry of the framework, with the highest in intensity being located at approximately 250 cm^{-1}. In ZIF-zni, there are more degenerate modes, and therefore there is a significant intensity at approximately 195 cm^{-1}. This region shows less significant features at 573 K, as the amorphous nature of the framework will negate any structural symmetry and result in such motions being so widely (randomly) distributed that no identifiable characteristic intensities are observed. It is worth noting that this region does not include the low-energy THz modes, reported in our previous work, involving phase-change and 'gate-opening' motions.[3] This spectral region (0–100 cm^{-1}) was out width the scope of the current experimental setup (Table 1).

For completeness, we also analyzed the mechanical properties of ZIF-zni (Table 2), for comparison to our previous elasticity work on the other Im containing ZIFs (ZIF-1, -2, -3 and -4).[18b] We performed the theoretical calculations at the same B3LYP level of theory as our previous work[18b] (explained in detail in the ESI†), so as to be able to comment on the quantitative mechanical property differences. The revised elasticity calculations reported in this work and in our recent work on the other four Im containing ZIF structures[18b] are an improved version to our initial calculations performed at the PBE level of theory.[21] Because of the higher density and increased symmetry of the ZIF-zni structure compared with ZIF-4, we observe an increase in the framework stiffness of the material (Young's moduli) by a factor of ~3. In addition, there is a two-fold increase in the resistance to shear strain through doubling of the maximum shear modulus (G_{max}), which can contribute to the mechanical destabilization of ZIF materials.[3,18b] The Poisson's ratio was also affected, in that it no longer possesses the 'cork-like' response (zero Poisson's ratio),

Table 2 Mechanical properties of ZIF-4 and ZIF-zni, derived from the elastic constants calculated by DFT at the B3LYP level of theory

Elastic property		ZIF-4[18b]	ZIF-zni
Young's modulus, E (GPa)	E_{max}	3.27	10.21
	E_{min}	2.17	6.82
	$A_E = E_{max}/E_{min}$	1.51	1.50
Shear modulus, G (GPa)	G_{max}	1.53	3.26
	G_{min}	0.77	2.30
	$A_G = G_{max}/G_{min}$	1.99	1.42
Linear compressibility, β (TPa^{-1})	β_{max}	241.2	29.5
	β_{min}	202.1	5.2
Poisson's ratio, ν	ν_{max}	0.41	0.49
	ν_{min}	0.06	0.32

in any direction, as is the case with ZIF-4 whose $\nu_{min} \approx$ zero. The values for Young's moduli agree with experimental nanoindentation values,[10] with the experimental E_{max} of ZIF-zni in the $\langle 001 \rangle$ direction ~9 GPa, and the experimental $E_{\langle 100 \rangle} \approx 8$ GPa (DFT value from this work, $E_{\langle 100 \rangle} = 8.6$ GPa).

In conclusion, the thermally induced amorphization of ZIF-4 into a-ZIF and its subsequent recrystallization upon additional heating to transform into ZIF-zni has been followed *in situ* using synchrotron Far-IR spectroscopy for the first time. We have demonstrated how vibrational spectroscopy can be used to gain a better understanding of how thermal stimulus can affect the stability of framework materials. Our work confirms the nature of each different vibrational motion and makes the connection between the flexibility (mechanical compliance) of the Zn–N tetrahedral moieties and the likelihood of thermal-induced amorphization. We have been able to measure the thermal stability to amorphization *via* an observed spectral shift in relation to the vibrational motions resulting from the polyhedral deformations and encourage future work in this area to test its wider applicability. In relation, we would expect other ZIF structures that possess the unsubstituted Im organic linker (*e.g.* ZIF-1, -2, -3, and -10) to have a similar thermal response to that reported for ZIF-4 in this work ($X_R = 0.045\ cm^{-1}\ K^{-1}$). It is also of great interest to further this research into MOFs with different metal polyhedra coordination, such as the high stability UiO series[22] and the isoreticular MIL-140 series.[23]

M. R. R. would like to thank the UK Engineering and Physical Sciences Research Council (EPSRC) for a DTA post-graduate scholarship and an additional scholarship from the Science and Technology Facilities Council (STFC) CMSD Award 13-05. M. R. R. would also like to thank the EPSRC for a Doctoral Prize Fellowship. The experimental work was performed at Diamond through beamtime (SM10215) on the B22 MIRIAM beamline. We thank the Rutherford Appleton Laboratory for access to the SCARF cluster. T. D. B. thanks the Royal Society for a University Research Fellowship.

Notes and references

1 (*a*) H. Furukawa, K. E. Cordova, M. O'Keeffe and O. M. Yaghi, *Science*, 2013, **341**, 1230444; (*b*) H. C. Zhou, J. R. Long and O. M. Yaghi, *Chem. Rev.*, 2012, **112**, 673–674; (*c*) M. R. Ryder and J. C. Tan, *Mater. Sci. Technol.*, 2014, **30**, 1598–1612.
2 (*a*) L. Sarkisov, R. L. Martin, M. Haranczyk and B. Smit, *J. Am. Chem. Soc.*, 2014, **136**, 2228–2231; (*b*) A. Schneemann, V. Bon, I. Schwedler, I. Senkovska, S. Kaskel and R. A. Fischer, *Chem. Soc. Rev.*, 2014, **43**, 6062–6096.
3 M. R. Ryder, B. Civalleri, T. D. Bennett, S. Henke, S. Rudic, G. Cinque, F. Fernandez-Alonso and J. C. Tan, *Phys. Rev. Lett.*, 2014, **113**, 215502.
4 K. S. Park, Z. Ni, A. P. Cote, J. Y. Choi, R. Huang, F. J. Uribe-Romo, H. K. Chae, M. O'Keeffe and O. M. Yaghi, *Proc. Natl. Acad. Sci. U. S. A.*, 2006, **103**, 10186–10191.
5 G. N. Greaves, F. Meneau, F. Kargl, D. Ward, P. Holliman and F. Albergamo, *J. Phys.: Condens. Matter*, 2007, **19**, 415102.
6 M. R. Ryder, B. Civalleri, G. Cinque and J. C. Tan, *CrystEngComm*, 2016, **18**, 4303–4312.
7 (*a*) Z. H. Dong and Y. Song, *J. Phys. Chem. C*, 2010, **114**, 1782–1788; (*b*) A. Greenaway, B. Gonzalez-Santiago, P. M. Donaldson, M. D. Frogley, G. Cinque, J. Sotelo, S. Moggach, E. Shiko, S. Brandani, R. F. Howe and P. A. Wright, *Angew. Chem., Int. Ed.*, 2014, **53**, 13483–13487.
8 (*a*) C. Gucuyener, J. van den Bergh, J. Gascon and F. Kapteijn, *J. Am. Chem. Soc.*, 2010, **132**, 17704–17706; (*b*) S. Aguado, G. Bergeret, M. P. Titus, V. Moizan, C. Nieto-Draghi, N. Bats and D. Farrusseng, *New J. Chem.*, 2011, **35**, 546–550; (*c*) P. Zhao, G. I. Lampronti, G. O. Lloyd, M. T. Wharmby, S. Facq, A. K. Cheetham and S. A. Redfern, *Chem. Mater.*, 2014, **26**, 1767–1769; (*d*) S. A. Moggach, T. D. Bennett and A. K. Cheetham, *Angew. Chem., Int. Ed.*, 2009, **48**, 7087–7089.
9 (*a*) C. Serre, S. Bourrelly, A. Vimont, N. A. Ramsahye, G. Maurin, P. L. Llewellyn, M. Daturi, Y. Filinchuk, O. Leynaud, P. Barnes and G. Ferey, *Adv. Mater.*, 2007, **19**, 2246–2251; (*b*) Y. Liu, J. H. Her, A. Dailly, A. J. Ramirez-Cuesta, D. A. Neumann and C. M. Brown, *J. Am. Chem. Soc.*, 2008, **130**, 11813–11818; (*c*) A. Ghoufi, A. Subercaze, Q. Ma, P. G. Yot, Y. Ke, I. Puente-Orench, T. Devic, V. Guillerm, C. Zhong, C. Serre, G. Ferey and G. Maurin, *J. Phys. Chem. C*, 2012, **116**, 13289–13295.
10 T. D. Bennett, A. L. Goodwin, M. T. Dove, D. A. Keen, M. G. Tucker, E. R. Barney, A. K. Soper, E. G. Bithell, J. C. Tan and A. K. Cheetham, *Phys. Rev. Lett.*, 2010, **104**, 115503.
11 D. A. Keen and M. T. Dove, *J. Phys.: Condens. Matter*, 1999, **11**, 9263–9273.
12 D. W. Lewis, A. R. Ruiz-Salvador, A. Gomez, L. M. Rodriguez-Albelo, F. X. Coudert, B. Slater, A. K. Cheetham and C. Mellot-Draznieks, *CrystEngComm*, 2009, **11**, 2272–2276.
13 E. O. Beake, M. T. Dove, A. E. Phillips, D. A. Keen, M. G. Tucker, A. L. Goodwin, T. D. Bennett and A. K. Cheetham, *J. Phys.: Condens. Matter*, 2013, **25**, 395403.
14 M. T. Wharmby, S. Henke, T. D. Bennett, S. R. Bajpe, I. Schwedler, S. P. Thompson, F. Gozzo, P. Simoncic, C. Mellot-Draznieks, H. Tao, Y. Yue and A. K. Cheetham, *Angew. Chem., Int. Ed.*, 2015, **54**, 6447–6451.
15 T. D. Bennett, J. C. Tan, Y. Yue, E. Baxter, C. Ducati, N. J. Terrill, H. H. Yeung, Z. Zhou, W. Chen, S. Henke, A. K. Cheetham and G. N. Greaves, *Nat. Commun.*, 2015, **6**, 8079.
16 (*a*) T. D. Bennett, P. Simoncic, S. A. Moggach, F. Gozzo, P. Macchi, D. A. Keen, J. C. Tan and A. K. Cheetham, *Chem. Commun.*, 2011, **47**, 7983–7985; (*b*) K. W. Chapman, G. J. Halder and P. J. Chupas, *J. Am. Chem. Soc.*, 2009, **131**, 17546–17547.
17 D.-Y. Kim, B. N. Joshi, J.-G. Lee, J.-H. Lee, J. S. Lee, Y. K. Hwang, J.-S. Chang, S. Al-Deyab, J. C. Tan and S. S. Yoon, *Chem. Eng. J.*, 2016, **295**, 49–56.
18 (*a*) A. U. Ortiz, A. Boutin, A. H. Fuchs and F. X. Coudert, *J. Phys. Chem. Lett.*, 2013, **4**, 1861–1865; (*b*) M. R. Ryder and J. C. Tan, *Dalton Trans.*, 2016, **45**, 4154–4161; (*c*) J. C. Tan, B. Civalleri, C. C. Lin, L. Valenzano, R. Galvelis, P. F. Chen, T. D. Bennett, C. Mellot-Draznieks, C. M. Zicovich-Wilson and A. K. Cheetham, *Phys. Rev. Lett.*, 2012, **108**, 095502.
19 G. Cinque, M. D. Frogley, K. Wehbe, J. Filik and J. Pikjanka, *Synchrotron Radiat. News*, 2011, **24**, 24–33.
20 (*a*) L. Vina, S. Logothetidis and M. Cardona, *Phys. Rev. B: Condens. Matter Mater. Phys.*, 1984, **30**, 1979–1991; (*b*) Y. C. Shen, P. C. Upadhya, E. H. Linfield and A. G. Davies, *Appl. Phys. Lett.*, 2003, **82**, 2350–2352.
21 J. C. Tan, B. Civalleri, A. Erba and E. Albanese, *CrystEngComm*, 2015, **17**, 375–382.
22 J. H. Cavka, S. Jakobsen, U. Olsbye, N. Guillou, C. Lamberti, S. Bordiga and K. P. Lillerud, *J. Am. Chem. Soc.*, 2008, **130**, 13850–13851.
23 (*a*) M. R. Ryder, B. Civalleri and J. C. Tan, *Phys. Chem. Chem. Phys.*, 2016, **18**, 9079–9087; (*b*) V. Guillerm, F. Ragon, M. Dan-Hardi, T. Devic, M. Vishnuvarthan, B. Campo, A. Vimont, G. Clet, Q. Yang, G. Maurin, G. Ferey, A. Vittadini, S. Gross and C. Serre, *Angew. Chem., Int. Ed.*, 2012, **51**, 9267–9271.

